Origin of the Half-Wavelength Errors in Microwave Measurements Using Through–Line Calibrations

P. Mark Buff, *Member, IEEE*, Jayesh Nath, *Member, IEEE*, and Michael B. Steer, *Fellow, IEEE*

***Abstract*—The through–line calibration family uses measurements of a through connection and an inserted line to determine the propagation constant of the line. This is typically used with measurements of a reflect standard to characterize fixturing errors. Subsequently, the *S*-parameters of a device under test are de-embedded. Measurement uncertainties occur at frequencies where the length of the line standard is an odd multiple of a half-wavelength. The origin of these errors is identified as fixture inconsistencies between the through and the line measurements. Error formulations are developed, and it is shown that a small fixturing error can be accounted for as a multiplicative transmission error. An error sensitivity function is developed and highlights the importance of fixture repeatability.**

***Index Terms*—De-embedding, genetic algorithm, propagation constant, through–line (TL) calibration, through–reflect–line (TRL).**

I. Introduction

THE THROUGH–reflect–line (TRL) technique [1] is a calibration procedure used for microwave measurements when classical standards such as open, short, and matched terminations cannot be realized. There are now a family of related techniques, here denoted as through–x–line (TxL) methods, with the commonality being the two-port measurement of a through connection and of the same structure with an inserted transmission line. These two measurements yield the complex propagation constant of the line but have errors that become evident at frequencies where the length of the line is an odd-integer multiple of a half-wavelength, i.e., the *critical* lengths [2], [3]. These errors affect the entire calibration and subsequent de-embedded measurements. A common frustration is that the size of these errors is seemingly unpredictable. The common strategy to mitigate these errors is to avoid using measurements where the line standard has an electrical length within 20° of a critical length.

It is well-known that the TxL half-wavelength peculiarities exist and are modeled using various approaches. Rolain *et al.* uses a mixed lumped-distributed perturbation model to ease the detection of errors seen in transmission line quantities [4]. Stumper uses a technique similar to that proposed here where sensitivity coefficients that describe "disturbed" scattering matrices for the calibration standards are derived [5], [6]. Additionally, efforts have been made to provide methods of correction for such errors using iterative and statistical techniques, such as those found in [7] and [8], respectively.

This paper discusses the origin of the half-wavelength errors in the TxL calibration family. It is shown that the errors are a result of limitations on the reproducibility of fixtures between the through and line measurements. An error analysis is presented that highlights the role of fixturing errors. It is shown that the errors can be captured by a transmission error in the fixtures, and the error is reduced if the line is lossy. The effects of fixture port coupling are not addressed in these formulations.

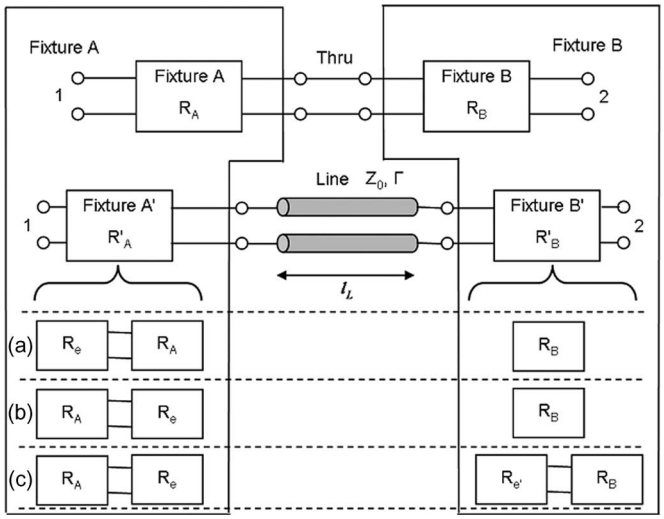

Fig. 1. TL components of TRL with fixture error introduced during the *line* measurement. Case (a) represents an asymmetrical fixture error in which R_e is located outside the fixture. Case (b) represents an asymmetrical fixture error in which R_e is located inside the fixture. Case (c) represents dual fixture errors, which are located inside the fixtures.

II. Through–Line Calibration

The through and line measurement structures include fixtures as well as the direct connection (for the through) and the inserted line (for the line) (see Fig. 1). The two-port measurements of these two structures yield the propagation constant $\gamma_L = \alpha + j\beta$ of the line [1]. The structures include error networks cascaded with their associated fixtures. For the through structure, the error networks between the ideal internal port of a

Manuscript received February 6, 2006; revised April 26, 2007. This work was supported by the U.S. Army Research Office under Grant DAAD19-02-1-0153.

P. M. Buff was with the Department of Electrical and Computer Engineering, North Carolina State University, Raleigh, NC 27695-7911 USA. He is currently with Vadum, Inc., Raleigh, NC 27606 USA.

J. Nath was with the Department of Electrical and Computer Engineering, North Carolina State University, Raleigh, NC 27695-7911 USA. He is currently with the Harris Stratex Networks, Morrisville, NC 27560 USA.

M. B. Steer is with the Department of Electrical and Computer Engineering, North Carolina State University, Raleigh, NC 27695-7911 USA.

Digital Object Identifier 10.1109/TIM.2007.904490

network analyzer and the desired measurement reference plane are designated as Fixture A at Port 1 and Fixture B at Port 2. For the line measurement, fixturing is reestablished (following the through measurement) with the line inserted. In general, the fixturing cannot be faithfully reproduced and therefore becomes Fixtures A′ and B′, respectively (see Fig. 1).

Following the original derivation [1], γ_L is developed using cascading matrices $\mathbf{R}$, each of which is related to the two-port scattering parameters $\mathbf{S}$ by

$$\mathbf{R} = \begin{bmatrix} R_{11} & R_{12} \\ R_{21} & R_{22} \end{bmatrix} = \begin{bmatrix} \dfrac{S_{12}S_{21} - S_{11}S_{22}}{S_{21}} & \dfrac{S_{11}}{S_{21}} \\ -\dfrac{S_{22}}{S_{21}} & \dfrac{1}{S_{21}} \end{bmatrix}. \quad (1)$$

Thus, the parameters describing the A and B fixtures are $\mathbf{S}_A$, $\mathbf{S}_B$ and $\mathbf{R}_A$, $\mathbf{R}_B$, respectively. The cascading matrix of the through is simply a unity matrix, and the line of length ℓ_L is described by

$$\mathbf{R}_L = \begin{bmatrix} e^{-\gamma_L \ell_L} & 0 \\ 0 & e^{\gamma_L \ell_L} \end{bmatrix}. \quad (2)$$

The characteristic impedance of the line is taken as the reference impedance Z_0 of the measurement system, however, the actual value of the line impedance is not required in determining γ_L. The cascading matrix of the through structure is

$$\mathbf{R}_t = \mathbf{R}_A \mathbf{R}_B \qquad (\text{Through}) \quad (3)$$

and the line structure (without fixturing errors such that $\mathbf{R}'_A = \mathbf{R}_A$ and $\mathbf{R}'_B = \mathbf{R}_B$) has the following cascading matrix:

$$\mathbf{R}_d = \mathbf{R}_A \mathbf{R}_L \mathbf{R}_B \qquad (\text{Line}). \quad (4)$$

Solving (3) for $\mathbf{R}_B$ and substituting into (4) yields what will be referred to as the through–line (TL) equation, i.e.,

$$\mathbf{T}\mathbf{R}_A = \mathbf{R}_A \mathbf{R}_L \quad (5)$$

where

$$\mathbf{T} = \mathbf{R}_d \mathbf{R}_t^{-1}. \quad (6)$$

Expanding the previous equations leads to the following system of equations:

$$t_{11}R_{A11} + t_{12}R_{A21} = R_{A11}e^{-\gamma_L \ell_L} \quad (7a)$$

$$t_{21}R_{A11} + t_{22}R_{A21} = R_{A21}e^{-\gamma_L \ell_L} \quad (7b)$$

$$t_{11}R_{A12} + t_{12}R_{A22} = R_{A12}e^{\gamma_L \ell_L} \quad (7c)$$

$$t_{21}R_{A12} + t_{22}R_{A22} = R_{A22}e^{\gamma_L \ell_L} \quad (7d)$$

which upon solution yields [1]

$$\gamma_L = \frac{1}{2\ell_L} \ln\left(\frac{t_{11} + t_{22} \pm \zeta}{t_{11} + t_{22} \mp \zeta}\right) \quad (8)$$

where

$$\zeta = \left(t_{11}^2 - 2t_{11}t_{22} + t_{22}^2 + 4t_{21}t_{12}\right)^{1/2}. \quad (9)$$

III. Insertion of Fixture Error

Errors in the repeatability of the fixtures can be described by an inserted two-port network, and three of the possible error configurations are considered here, as shown in Fig. 1. The errors are represented variously as follows: in Case (a), as an asymmetrical error located outside the fixture; in Case (b), as an asymmetrical error located inside the fixture; and in Case (c), as a dual fixture error located inside the fixtures. In the following, we solve for the propagation constant incorporating the impact of various error configurations.

Case (a)

In Case (a) shown in Fig. 1, Fixture A is preceded by a two-port error with cascading parameters, i.e.,

$$R_e = \begin{bmatrix} \Lambda_{A11} & \Lambda_{A12} \\ \Lambda_{A21} & \Lambda_{A22} \end{bmatrix} \quad (10)$$

and the TL equation (5) becomes

$$\mathbf{T}\mathbf{R}_A = \mathbf{R}_{eA}\mathbf{R}_L \quad (11)$$

where

$$\mathbf{R}_{eA} = \mathbf{R}_e \mathbf{R}_A. \quad (12)$$

The aim here is to proceed with a new derivation of γ_L that incorporates the effect of error. Matters can be simplified by noting that fixturing error can be expected to be small and, in practice, is largely attributable to the difficulty of precisely establishing the location of the reference planes. Thus, a small transmission two-port error is introduced with cascading parameters, i.e.,

$$\mathbf{R}_e = \begin{bmatrix} e^{-\Delta} & 0 \\ 0 & e^{\Delta} \end{bmatrix} \quad (13)$$

where Δ is complex. The quantity Δ does not necessarily correspond to delay and does not need to vary smoothly with respect to frequency. (As expected, $\mathbf{R}_e$ is an identity matrix when the error is zero, i.e., $\Delta = 0$.) As will be shown in Section V, this fixturing error fully captures the error as far as γ extraction is concerned. With (13), (12) becomes

$$\mathbf{R}_{eA} = \begin{bmatrix} R_{A11}e^{-\Delta} & R_{A12}e^{-\Delta} \\ R_{A21}e^{\Delta} & R_{A22}e^{\Delta} \end{bmatrix} \quad (14)$$

and the TL equations are now given as follows:

$$e^{\Delta}(t_{11}R_{A11} + t_{12}R_{A21}) = R_{A11}e^{-\gamma_L \ell_L} \quad (15a)$$

$$e^{-\Delta}(t_{21}R_{A11} + t_{22}R_{A21}) = R_{A21}e^{-\gamma_L \ell_L} \quad (15b)$$

$$e^{\Delta}(t_{11}R_{A12} + t_{12}R_{A22}) = R_{A12}e^{\gamma_L \ell_L} \quad (15c)$$

$$e^{-\Delta}(t_{21}R_{A12} + t_{22}R_{A22}) = R_{A22}e^{\gamma_L \ell_L}. \quad (15d)$$

Solving these as before produces

$$\gamma_L = \frac{1}{2\ell_L} \ln\left(\frac{e^{\Delta}t_{11} + e^{-\Delta}t_{22} \pm \Psi}{e^{\Delta}t_{11} + e^{-\Delta}t_{22} \mp \Psi}\right) \tag{16}$$

where

$$\Psi = \left(e^{2\Delta}t_{11}^2 - 2t_{11}t_{22} + t_{22}^2 e^{-2\Delta} + 4t_{21}t_{12}\right)^{1/2}. \tag{17}$$

Case (*b*)

With the error network located inside Fixture A (Case (b) in Fig. 1) and using $\mathbf{R}_e$ from (13), the TL equation becomes

$$\mathbf{T}\mathbf{R}_A = \mathbf{R}_{Ae}\mathbf{R}_L \tag{18}$$

where

$$\mathbf{R}_{Ae} = \mathbf{R}_A\mathbf{R}_e. \tag{19}$$

These error variants can become useful when there is a need to solve for either a single- or dual-ended fixture error. For the single-ended error of Case (b), the equations to solve are given as follows:

$$t_{11}R_{A11} + t_{12}R_{A21} = R_{A11}e^{-\Delta}e^{-\gamma_L\ell_L} \tag{20a}$$
$$t_{21}R_{A11} + t_{22}R_{A21} = R_{A21}e^{-\Delta}e^{-\gamma_L\ell_L} \tag{20b}$$
$$t_{11}R_{A12} + t_{12}R_{A22} = R_{A12}e^{\Delta}e^{\gamma_L\ell_L} \tag{20c}$$
$$t_{21}R_{A12} + t_{22}R_{A22} = R_{A22}e^{\Delta}e^{\gamma_L\ell_L}. \tag{20d}$$

Solving the system of equations in the same manner as before produces

$$\gamma_L = \frac{1}{2\ell_L}\left[\ln\left(\frac{t_{11} + t_{22} \pm \zeta}{t_{11} + t_{22} \mp \zeta}\right) - 2\Delta\right] \tag{21}$$

where ζ is the same as that in (9).

Case (*c*)

Case (c) contains two error networks as follows: the first being that described by (13) and the second being denoted by

$$\mathbf{R}_{e'} = \begin{bmatrix} e^{-\Delta'} & 0 \\ 0 & e^{\Delta'} \end{bmatrix}. \tag{22}$$

The propagation constant becomes

$$\gamma_L = \frac{1}{2\ell_L}\left[\ln\left(\frac{-2\,t_{11}t_{21} - t_{12}t_{11} + t_{12}t_{22} \pm t_{12}\zeta}{-2\,t_{11}t_{21} - t_{12}t_{11} + t_{12}t_{22} \mp t_{12}\zeta}\right) - 2(\Delta + \Delta')\right]. \tag{23}$$

In summary, in the three cases it is observed that the transmission error introduces an error in the extraction of γ_L. In effect, there is an uncertainty in the electrical length.

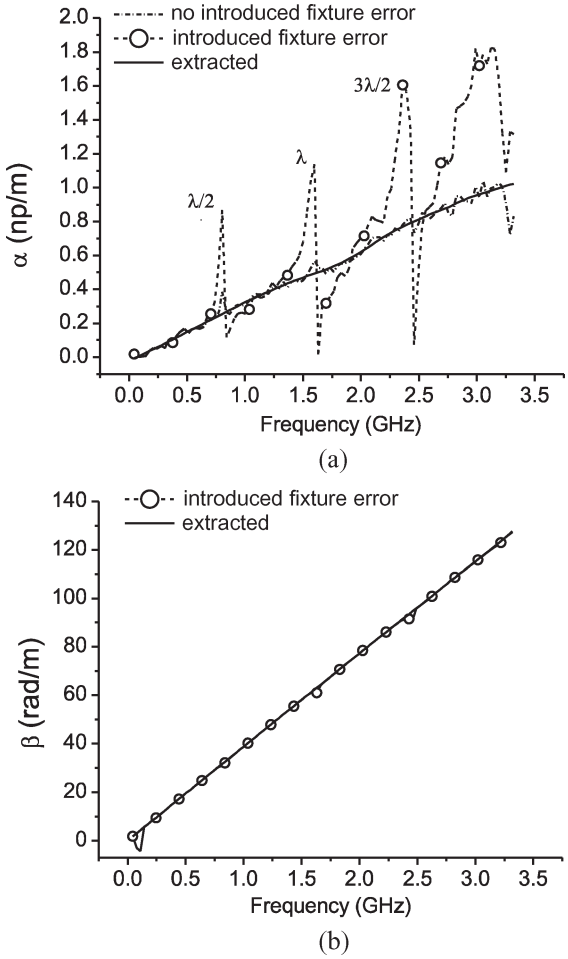

Fig. 2. Propagation constant extracted from measurements. (a) α. (b) β. The curves are α for the nonerrored line, and α and β for the errored line and the fits.

IV. Fixture Error Investigation

For verification of the aforementioned error formulation, a series of 50-Ω microstrip lines is fabricated on a 62-mil-thick FR-4 laminate substrate with a dielectric constant of 4.6 and a loss tangent of 0.016. Two sets of measurements were performed yielding *errored* and *nonerrored* measurements. In one set, i.e., the nonerrored measurements, the through and line structures were measured with the fixtures reproduced as faithfully as possible. Fixtures consisted of a SubMiniature version A connector and a short section of microstrip line that is approximately 1 cm long. The components of the propagation constant that were extracted from these measurements are shown in Fig. 2 and designated as "no introduced fixture error." In the second set, which is the errored measurements, the error was deliberately introduced in Fixture A during the line measurement by placing a small piece of substrate on top of the microstrip line that composes Fixture A. This altered the two-port describing the fixture making it dissimilar to that of the through measurement. The components of the propagation constant that were extracted from these measurements are also shown in Fig. 2 and designated as "introduced fixture error." In both cases, β in Fig. 2(b) is reasonably smooth, but errors are seen

clearly in α [Fig. 2(a)]. In the measurements with no fixture error, the glitches in α at the half-wavelength frequencies are small. They are greatly exaggerated however with the errored measurements where the fixture error was introduced. While the error is nominally equivalent at all frequencies, the error clearly has the most significant impact at half-wavelength frequencies. The "extracted" results shown in Fig. 2 were produced using an optimization technique with the results of (16). A genetic algorithm was employed to fit the errored propagation constant γ_L to a smoothed version of the nonerrored γ_L, producing a fit with an average error of $2 \cdot 10^{-5}$ and a total error of 0.002. The significance of this good fit is that it indicates that the transmission error described by R_e [(13)] fully describes the fixture error.

V. Fixture Error Capture

In the TxL calibration procedure, fixturing error is reflected in inaccuracies in extracting fixture scattering parameters. The purpose of this section is to identify the contributions of the transmission errors captured by Δ to the effective fixture two-port parameters. The errored fixture is defined in terms of S-parameters in the following form:

$$\begin{bmatrix} S_{11A}(1+\delta_{11A}) & S_{12A}(1+\delta_{12A}) \\ S_{21A}(1+\delta_{21A}) & S_{22A}(1+\delta_{22A}) \end{bmatrix} \tag{24}$$

or as a cascading matrix as

$$\mathbf{R} = \begin{bmatrix} R_{11} & R_{12} \\ R_{21} & R_{22} \end{bmatrix} \tag{25}$$

where

$$\begin{aligned} R_{11} &= \frac{S_{A12}(1+\delta_{A12})S_{A21}(1+\delta_{A21})}{S_{A21}(1+\delta_{A21})} \\ &\quad - \frac{S_{A11}(1+\delta_{A11})S_{A22}(1+\delta_{A22})}{S_{A21}(1+\delta_{A21})} \\ R_{12} &= \frac{S_{A11}(1+\delta_{A11})}{S_{A21}(1+\delta_{A21})} \\ R_{21} &= -\frac{S_{A22}(1+\delta_{A22})}{S_{A21}(1+\delta_{A21})} \\ R_{22} &= \frac{1}{S_{A21}(1+\delta_{A21})}. \end{aligned}$$

It is in this form that we ultimately want to represent the fixture error described by $\mathbf{R}_{eA}$ or $\mathbf{R}_{Ae}$.

For Case (a), the desired error term $\mathbf{R}$ in (25) is equated to the cascading fixture error term $\mathbf{R}_{eA}$, leading to

$$\begin{bmatrix} R_{11} & R_{12} \\ R_{21} & R_{22} \end{bmatrix} = \begin{bmatrix} \dfrac{e^{-\Delta}(S_{A12}S_{A21} - S_{A11}S_{A22})}{S_{A21}} & \dfrac{e^{-\Delta}S_{A11}}{S_{A21}} \\ -\dfrac{e^{\Delta}S_{A22}}{S_{A21}} & \dfrac{e^{\Delta}}{S_{A21}} \end{bmatrix}. \tag{26}$$

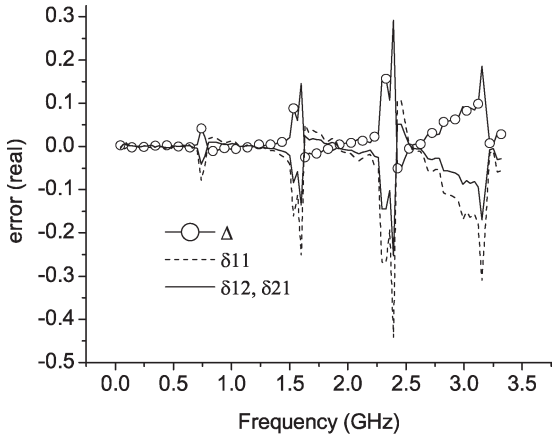

(a)

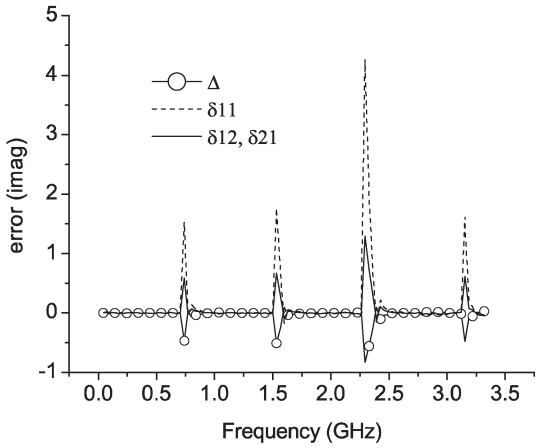

(b)

Fig. 3. Complex error needed to de-embed the *nonerrored* solution in terms of Δ and δ for the data in Fig. 2.

This produces the following governing relationship between the errored fixture *S*-parameters and the cascading fixture error term $\mathbf{R}_{eA}$ [(12)]:

$$\begin{bmatrix} \delta_{A11} & \delta_{A12} \\ \delta_{A21} & \delta_{A22} \end{bmatrix} = \begin{bmatrix} e^{-2\Delta} - 1 & e^{-\Delta} - 1 \\ e^{-\Delta} - 1 & 0 \end{bmatrix}. \tag{27}$$

When the fixture error term $\mathbf{R}_e$ is placed inside the fixture, as in Cases (b) and (c), then the matrix that relates $\mathbf{R}_A\mathbf{R}_e$ to the errored fixture *S*-parameters becomes

$$\begin{bmatrix} \delta_{A11} & \delta_{A12} \\ \delta_{A21} & \delta_{A22} \end{bmatrix} = \begin{bmatrix} 0 & e^{-\Delta} - 1 \\ e^{-\Delta} - 1 & e^{-2\Delta} - 1 \end{bmatrix}. \tag{28}$$

These formulations are required to associate the cascade error matrices of (16) and (21) to the errored *S*-parameters of the fixture. The resultant complex error quantities produced by the genetic algorithm needed to de-embed the nonerrored solution in terms of Δ, δ_{11}, δ_{12}, and δ_{21} are shown in Fig. 3. This demonstrates that the transmission error represented by (13) fully captures the errors in fixture inconsistencies between the through and line measurements.

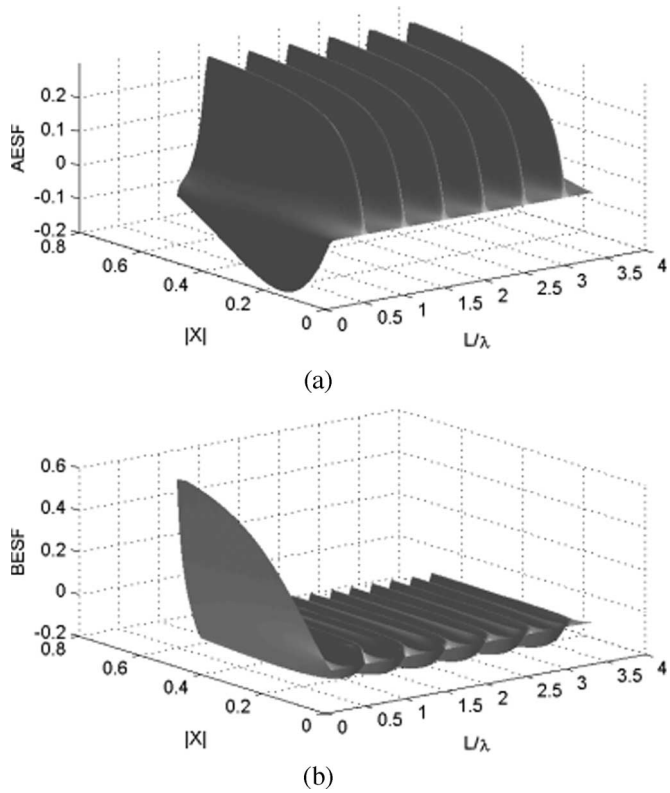

Fig. 4. Fixture error for varying Δ magnitude for (a) α and (b) β.

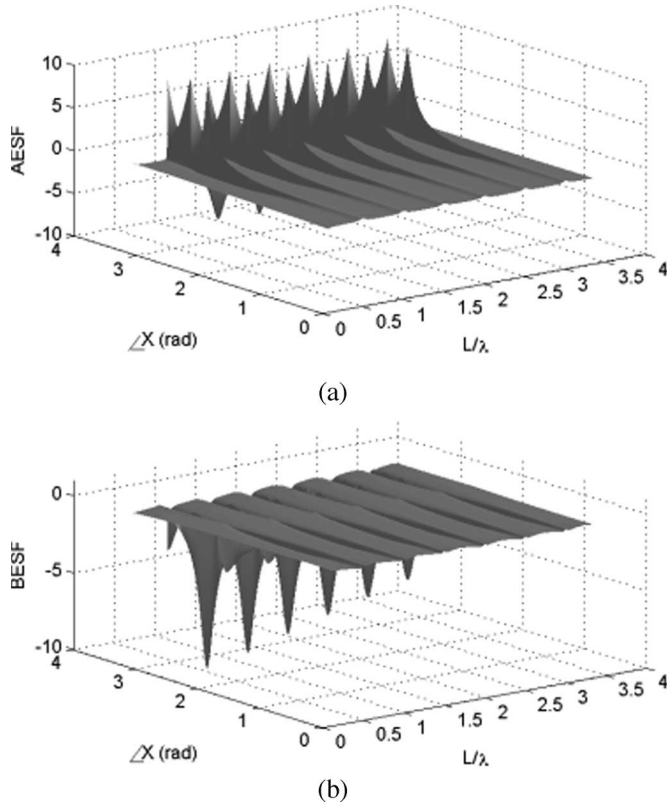

Fig. 5. Fixture error for varying Δ angle for (a) α and (b) β.

VI. Sensitivity Analysis

The errors in TxL calibration result in significantly enhanced errors at frequencies corresponding to the length of the line being multiples of a half-wavelength. We explore this further by developing the sensitivity of the extracted propagation constant. This is performed by analyzing how γ_L in (16) varies as a function of Δ by taking the derivative with respect to the fixture error, producing the error sensitivity function (ESF) as follows:

$$\text{ESF} = \frac{\partial \gamma_L}{\partial \Delta} = \frac{4\left(t_{11}e^{\Delta} - t_{22}e^{-\Delta}\right)(t_{11}t_{22} - t_{21}t_{12})}{l\Psi(t_{11}e^{\Delta} + t_{22}e^{-\Delta} + \Psi)(-t_{11}e^{\Delta} - t_{22}e^{-\Delta} + \Psi)}. \tag{29}$$

ESF is a function of Δ and can be separated into its real and imaginary components as follows: α ESF and β ESF. In Fig. 4, the magnitude of δ is varied while the angle is kept constant at 0 rad so that the sensitivity of γ_L to error can be accessed. Additionally, in Fig. 5 the magnitude of δ is held constant at 0.1 while the angle is varied from 0 to π. The ESF is obviously dependent on the measured quantities T. Figs. 4 and 5 demonstrate a dramatic increase in sensitivity to transmission error at frequencies corresponding to multiples of a half-wavelength.

VII. Conclusion

It has been shown how fixture variation in the transition from the *through* to the *line* in TL calibration procedures can lead to the well-known $\lambda/2$ error. It was shown that the impact of errors in fixture reproducibility on propagation constant extraction can be accounted for by a transmission error. An ESF that allows the sensitivity of γ_L to fixture variation error to be assessed has been presented. This also indicates a high sensitivity to fixture errors at frequencies corresponding to multiples of a half-wavelength.

References

[1] F. Engen and C. A. Hoer, "Thru–reflect–line: An improved technique for calibrating the dual six-port automatic network analyzer," *IEEE Trans. Microw. Theory Tech.*, vol. MTT-27, no. 12, pp. 987–993, Dec. 1979.

[2] C. A. Hoer, "Some questions and answers concerning air lines as impedance standards," in *Proc. 29th Autom. RF Tech. Group Conf.*, 1987, pp. 161–173.

[3] C. A. Hoer, "Choosing line lengths for calibrating network analyzers," *IEEE Trans. Microw. Theory Tech.*, vol. MTT-31, no. 1, pp. 76–78, Jan. 1983.

[4] Y. Rolain, W. Van Moer, J. Jargon, and D. DeGroot, "On peculiarities of S-parameters measurements," in *Proc. 65th ARFTG Microw. Meas. Conf.*, Long Beach, CA, Jun. 2005, pp. 89–95.

[5] U. Stumper, "Influence of nonideal LRL or TRL calibration elements on VNA S-parameter measurements," in *Adv. Radio Sci. (Kleinheubacher Berichte)*, vol. 3, 2005, pp. 51–58. [Online]. Available: http://www.copernicus.org/URSI/ars/3/ars-3-51.pdf

[6] U. Stumper, "Uncertainty of VNA S-parameter measurement due to nonideal TRL calibration items," *IEEE Trans. Instrum. Meas.*, vol. 55, no. 2, pp. 676–679, Apr. 2005.

[7] D. Williams, C. Wang, and U. Arz, "An optimal multiline TRL calibration algorithm," *IEEE Trans. Microw. Theory Tech.*, vol. 51, no. 6, pp. 1205–1215, Jun. 2003.

[8] D. DeGroot, "Correction for nonlinear vector network analyzer measurements using a stochastic multiline reflect method," in *IEEE MTT-S Int. Microw. Symp. Dig.*, Fort Worth, TX, Jun. 2004, vol. 3, pp. 1735–1738.

P. Mark Buff (S'02–M'06) received the B.S. degree in electrical engineering, the M.S. degree in computer engineering, and the Ph.D. degree in electrical engineering from North Carolina State University, Raleigh, in 1994, 2003, and 2006, respectively.

In 2004, he cofounded Vadum, Inc., Raleigh, an emerging high-technology U.S. Department of Defense contracting start-up, where he is currently the Chief Operating Officer and Principal Investigator. His research interests include novel antenna designs for military applications, intelligent jamming techniques, and electromagnetic instrumented surrogates.

Dr. Buff is a member of the IEEE Microwave Theory and Techniques Society and the IEEE Antennas and Propagation Society. He is also the Secretary of the IEEE Antennas and Propagation/Components, Packaging, and Manufacturing Technology/Microwave Theory and Techniques/Electron Devices Societies (ACME) Chapter, Raleigh.

Jayesh Nath (S'99–M'07) received the B.E. degree (with honors) in electronics and communication engineering from the Birla Institute of Technology-Mesra, Ranchi, India, in 2001, and the Ph.D. degree in electrical engineering (with a minor in materials science and engineering) from North Carolina State University, Raleigh, in 2006.

From February 2006 to January 2007, he was with the Microwave Communication Division, Harris Corporation, Morrisville, NC, as a Senior Member Technical Staff in the RF Conversion Technology Group. Since January 2007 he has been with Harris Stratex Networks, Morrisville, as Senior Member Technical Staff. His main research interests include the design, characterization, and modeling of tunable RF and microwave devices based on ferroelectrics, electromagnetic design and modeling, measurement and calibration techniques, integrated passives, and 3-D packaging.

Dr. Nath is a member of the IEEE Microwave Theory and Techniques Society (IEEE MTT-S), the IEEE Antennas and Propagation Society, and the IEEE Components, Packaging and Manufacturing Technology Society.

Michael B. Steer (S'76–M'82–SM'90–F'99) received the B.E. and Ph.D. degrees in electrical engineering from the University of Queensland, Brisbane, Australia, in 1976 and 1983, respectively.

In 1983, he joined the Department of Electrical and Computer Engineering, North Carolina State University, Raleigh, where he is currently a Professor. In 1999 and 2000, he was a Professor with the School of Electronic and Electrical Engineering, The University of Leeds, Leeds, U.K., where he was the Director of the Institute of Microwaves and Photonics and held the Chair in Microwave and Millimeterwave Electronics. He has authored more than 300 publications and coauthored *Foundations of Interconnect and Microstrip Design* (Wiley, 2000).

Prof. Steer was the Secretary of the IEEE Microwave Theory and Techniques Society (IEEE MTT-S) in 1997 and a member of its Administrative Committee from 1998 to 2000. He was the Editor-in-Chief of the IEEE TRANSACTIONS ON MICROWAVE THEORY AND TECHNIQUES (2003–2006).